

Article

Reactivity of Au/La_{1-x}Sr_xCr_{1-y}Ni_yO_{3-δ} toward Oxidative Coupling of Methane for C₂ and C₃ Hydrocarbons Production

Hatairat Worrathon¹, Wisitsree Wiyaratn^{2*}, Suttichai Assabumrungrat³,
and Navadol Laosiripojana¹

¹ The Joint Graduate School of Energy and Environment, CHE Center for Energy Technology and Environment, King Mongkut's University of Technology Thonburi, Bangkok, 10140, Thailand

² Faculty of Industrial Education and Technology, King Mongkut's University of Technology Thonburi, Bangkok, 10140, Thailand

³ Centre of Excellence in Catalysis and Catalytic Reaction Engineering, Department of Chemical Engineering, Faculty of Engineering, Chulalongkorn University, Bangkok 10330, Thailand

*E-mail: Wisitsree.Wiy@kmutt.ac.th (Corresponding author)

Abstract. La_{0.8}Sr_{0.2}Cr_{0.9}Ni_{0.1}O₃ (LSCN) perovskite was calcined in hydrogen atmosphere (LSCN-H₂) that provides better activity than LSCN-air. The doping of Au (as Au/LSCN-H₂) improved the catalyst stability toward oxidative coupling of methane (OCM) reaction by increasing the resistance of carbon formation on catalyst surface during the reaction. The suitable CH₄:O₂ ratio appeared to be 2:1, from which 5.8%, 29.9%, 8.1%, and 5.8% of C₂H₄, C₂H₆, C₃H₆, and C₃H₈ can be produced respectively. Importantly, the addition of CO₂ can significantly promote the yield of C₃H₈ produced, from which the suitable CH₄:CO₂ ratio was observed to be 1:2 (with or without O₂ presenting).

Keywords: LSCN Perovskite, gold, oxidative coupling of methane.

ENGINEERING JOURNAL Volume 18 Issue 4

Received 5 April 2013

Accepted 14 November 2013

Published 16 October 2014

Online at <http://www.engj.org/>

DOI:10.4186/ej.2014.18.4.1

1. Introduction

Lacking of fossil fuels and the current global warming crisis drive the researchers to find new energy resources, which are of high efficiency and environmental friendly. Solid oxide fuel cell (SOFC) is known as an energy device that can generate clean electrical energy with high efficiency for power generation application. Nevertheless, the main barrier of SOFC is its high investment cost, which results in the expensive electricity production. Therefore, the new approach for SOFC operation by integrating the electricity generation with high-value chemical synthesis as called "SOFC cogeneration with chemical production" is currently of interest [1, 2].

It is known that, along with hydrogen (H_2) and synthesis gas (the mixture of CO and H_2), the most interesting primary fuel for SOFC is methane (CH_4) because it is an abundant component in conventional natural gas and could be internally reformed at the anode side of SOFC, as called Direct Internal Reforming (DIR) operation. Importantly, it is well established that CH_4 can also be converted to valuable chemicals such as C_2 hydrocarbons (ethylene and ethane), which are useful chemical compounds in petrochemical industries via the oxidative coupling of methane (OCM) reaction [3, 4]. Therefore, the integration of SOFC cogeneration for electricity generation and C_2 hydrocarbons production via OCM reaction is an attractive approach for reducing the total cost of electricity generation [5-7]. It is well established that the use of suitable catalyst at the electrode of SOFC is the key issue for achieving the good SOFC cogeneration performance. Recently, several types of catalyst for OCM reaction have been studied and reported, from which the suitable catalysts for this reaction include SrF_2/Nd_2O_3 , $Mn/Na_2WO_4/SiO_2$, La_2O_3 , $LaAlO_3$, $LaCoO_3$, $LaCrO_3$, $Ba_xSr_{1-x}TiO_3$, $SrTi_{1-x}Li_xO_3$ and Au/LSM [8-17]. Among these catalysts, the use of perovskite material (ABO_3) as the catalyst as well as the support for the OCM reaction has been widely reported to enhance the good activity in term of product yield and product selectivity [18-27]. Importantly, the properties of perovskite material can tolerate a wide variety of composition and constituent elements by the main structure unchanged; hence perovskite material has the possibility to improve the properties by partial substitution of cations and can be used at high temperature conditions. Among perovskite material, $LaCrO_3$ -based perovskite material has been widely investigated for SOFC applications i.e. as an anode component and as an internal reforming catalyst. Nevertheless, it is well known that pure lanthanum chromite shows a decrease in mechanical strength under reducing conditions as well as phase segregation in the microstructure due to the evaporation of gaseous CrO_3 from $LaCrO_3$ particles at high temperature; the partial substitution of Cr on the B-site by Ni (Cr/Ni of 0.9/0.1) has been reported to improve the structural stability without a significant decrease in its catalytic reactivity. Furthermore, the partial substitution of the A-site cation with alkaline earths (i.e., Sr) has been found to increase the catalytic reactivity of $LaCrO_3$ -based perovskite material due to the stabilizing of the B-site cation as well as the introducing of structural defects e.g., oxygen vacancies. Therefore, $La_{1-x}Sr_xCr_{1-y}Ni_yO_{3-\delta}$ was selected as the catalyst for OCM reaction in the present work. In addition, the effect of gold (Au) doping over $La_{1-x}Sr_xCr_{1-y}Ni_yO_{3-\delta}$ on the OCM performance was also investigated since it is known that Au can promote the catalytic activity of various thermochemical reactions.

In the present work, $La_{1-x}Sr_xCr_{1-y}Ni_yO_{3-\delta}$ was synthesized by co-precipitation techniques, which enables to produce the material with nano-particle size and high surface area. The effects of Au doping as well as the catalyst pretreatment condition (i.e. calcination in air and/or hydrogen) on the catalytic OCM activity under various conditions were performed.

2. Experimental

2.1. Catalyst Preparation and Characterization

$La_{0.8}Sr_{0.2}Cr_{0.9}Ni_{0.1}O_3$ perovskite was prepared by co-precipitation technique. $La(NO_3)_3$, $Sr(NO_3)_2$, $Cr(NO_3)_3 \cdot 9H_2O$ and $Ni(NO_3)_2 \cdot 6H_2O$ were used as starting materials. Initially, stoichiometric amounts of metal nitrates were dissolved in deionized water. The mixture solution was stirred at room temperature and then its pH was adjusted to 10-11 with the addition of ammonia solution. The precipitate was aged in the original solution for 24 hours. After that, the precipitate was filtered, washed with deionized water until pH 7, and dried overnight at $100^\circ C$. Then, the dried precipitate was ground to be powder form. The dried precipitate was ground and calcined in different atmospheric conditions i.e. air and hydrogen ($10\% H_2/He$) at $900^\circ C$ for 3 hours. This process was started from room temperature to $900^\circ C$ with a heating rate of

20°C·min⁻¹. Then 3 wt% Au of HAuCl₄ (Tetrachloroauric (III) acid) was deposited on La_{0.8}Sr_{0.2}Cr_{0.9}Ni_{0.1}O₃ perovskite by deposition-precipitation technique integrated with ultrasound in an ultrasonic bath for 6 hours. The dispersion was filtered, washed with deionized water until pH equal to 7, and dried at 100°C. Finally, the dried sample was heated at 300°C for 4 hours in air atmosphere.

The synthesized catalysts were determined their physical properties by various techniques. Surface area and pore size were determined by BET method. The crystalline phase was identified by X-Ray Diffraction (XRD). Scanning Electron Microscopy (SEM) was also used to examine the surface morphology of synthesized catalyst and gold particle size was determined by Transmission Electron Microscopy (TEM).

2.2. Catalytic Activity Testing

A schematic diagram of the experimental system of OCM is shown in Fig. 1. This system was constructed with three main sections i.e., supplied gases, reaction zone, and analysis section. The supplied gases were composed of 99.99% helium, 5% methane, and 10% oxygen diluted in helium. They were used without further purification. The ratio of mixing gases depended on the purpose of each experiment.

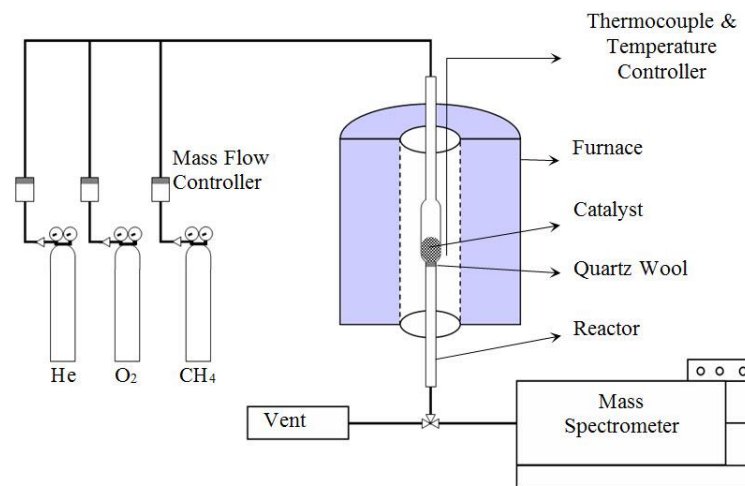


Fig. 1. Schematic diagram of oxidative coupling of methane system.

The reaction was carried out in a tubular quartz reactor filled with 100 mg of selected sample and small amount of quartz wool. The reactor was vertically mounted inside a furnace. Gas mixture between methane and oxygen diluted in helium were allowed to continually flow into the reaction zone at a total flow rate 200 cm³·min⁻¹. The reactions were studied in temperature range of 800-900°C (heating rate of 20°C·min⁻¹) and held around 3 hours until equilibrium was reached. The study of OCM is shown in Table 1. It is noted that the effects of CH₄:O₂ inlet ratio and carbon dioxide (CO₂) addition on the catalytic performance were also determined. After reaction, the composition of effluent gas was analyzed by an online mass spectrometer (Pfeiffer Vacuum; Omnistar™ GSD 301). In the present work, the catalytic performance was evaluated in terms of reactant conversion and product yields using the following equations:

Conversion of reactants

$$X_R = \left(\frac{R_{in} - R_{out}}{R_{in}} \right) \times 100 \quad (1)$$

where R is concentration of CH₄, O₂, or CO₂

Product yields

- For the reaction of CH₄ + O₂

$$Y_{C_2} = \left(\frac{2 * C_{2,out}}{CH_{4,in}} \right) \times 100 \quad (2)$$

$$Y_{C_3} = \left(\frac{3 * C_{3,out}}{CH_{4,in}} \right) \times 100 \quad (3)$$

- For the reactions of $CH_4 + CO_2$ and $CH_4 + O_2 + CO_2$

$$Y_{C_2} = \left(\frac{2 * C_{2,out}}{CH_{4,in} + CO_{2,in}} \right) \times 100 \quad (4)$$

$$Y_{C_3} = \left(\frac{3 * C_{3,out}}{CH_{4,in} + CO_{2,in}} \right) \times 100 \quad (5)$$

Table 1. The studied operating parameters of OCM reaction.

Parameter	Data
CH ₄ :O ₂ ratio	2:1, 3:1, 4:1, 5:1, 6:1
Operating temperature	800, 825, 850, 875, 900°C
Atmospheric condition	Oxidizing atmosphere (10%O ₂ /He), Reducing atmosphere (He)
Aging condition	No aging, Aging with helium flow for 13 hours at 900°C
CO ₂ adding	CH ₄ :O ₂ :CO ₂ ratio = 2:1:4, 2:1:2, 2:1:1 CH ₄ :CO ₂ ratio = 1:2, 1:1, 2:1

3. Result and Discussion

3.1. Catalyst characteristics

The prepared materials consisted of La_{0.8}Sr_{0.2}Cr_{0.9}Ni_{0.1}O₃ calcined under air atmosphere (LSCN-air), La_{0.8}Sr_{0.2}Cr_{0.9}Ni_{0.1}O₃ calcined under hydrogen atmosphere (LSCN-H₂), Au supported on La_{0.8}Sr_{0.2}Cr_{0.9}Ni_{0.1}O₃ calcined under air atmosphere (Au/LSCN-air), and Au supported on La_{0.8}Sr_{0.2}Cr_{0.9}Ni_{0.1}O₃ calcined under hydrogen atmosphere (Au/LSCN-H₂). These materials were characterized their properties by various techniques. The specific surface area, pore volume, and pore size of four synthesized catalysts were determined by BET measurement. The results in Table 2 suggest that LSCN-H₂ provides the material with higher specific surface area than LSCN-air. Furthermore, the total pore volume of the catalyst calcined under hydrogen flow is relatively higher, whereas the pore size diameter is lower. According to perovskite-based materials with gold deposited, the specific surface area and total pore volume slightly decrease when compared to the un-doped gold samples.

Table 2. The results of BET surface area and pore size analyzer.

Materials	Surface Area (m ² ·g ⁻¹)	Pore Volume (cm ³ ·g ⁻¹)	Pore Diameter (nm)
LSCN-air	3.6354	0.0790	86.96
LSCN-H ₂	7.2606	0.1037	57.16
Au/LSCN-air	2.0664	0.0291	95.27
Au/LSCN-H ₂	6.4967	0.0733	46.13

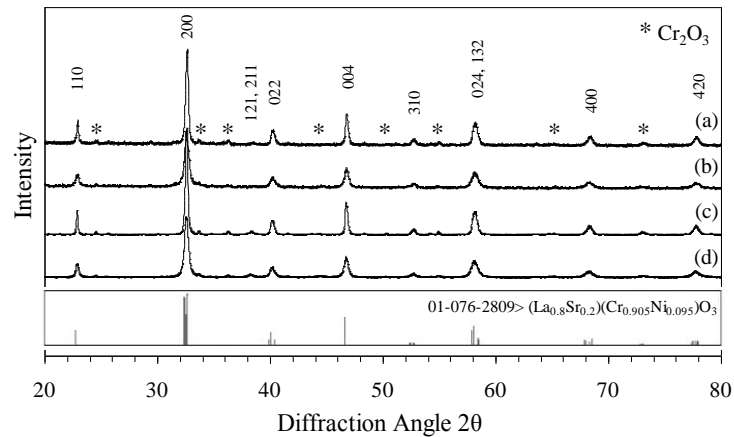


Fig. 2. XRD patterns of prepared samples; (a) LSCN-air, (b) LSCN-H₂, (c) Au/LSCN-air, and (d) Au/LSCN-H₂.

The synthesized materials were analyzed their crystalline phase by x-ray diffraction (XRD). As shown in Fig. 2, it can be identified that the perovskite-based materials prepared by co-precipitation technique have the same XRD pattern as $\text{La}_{0.8}\text{Sr}_{0.2}\text{Cr}_{0.905}\text{Ni}_{0.095}\text{O}_3$ (JCPDS #01-076-2809) which have orthorhombic structure. However, tiny peaks of chromium oxide phase (Cr_2O_3) can also be observed in the perovskite calcined under air atmosphere. This is different from the perovskite calcined under hydrogen atmosphere, which can not be observed Cr_2O_3 phase. Furthermore, phase of gold particle can not be showed in the structure of Au/LSCN-air and Au/LSCN-H₂. This was probably due to the deposition of small gold content in these materials.

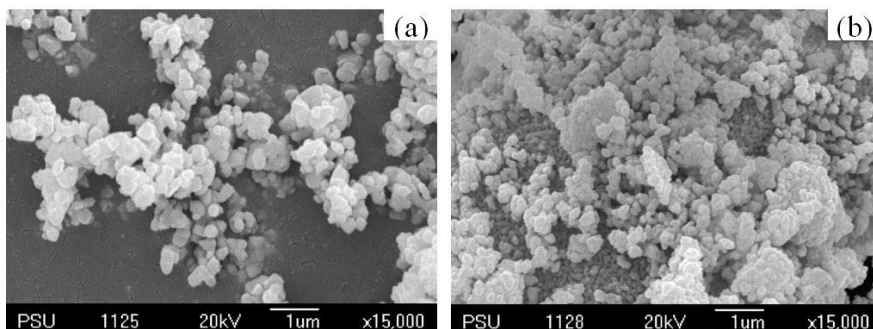


Fig. 3. Surface morphology of (a) LSCN-air and (b) LSCN-H₂.

The SEM micrographs in Fig. 3 show that the average particle size of the perovskite calcined in hydrogen is slightly smaller than the perovskite calcined in the air. The particle size of the perovskite calcined in hydrogen is in the range of 0.1-0.2 μm whereas the particle size of the perovskite calcined in air is in the range of 0.2-0.4 μm . Au/ $\text{La}_{0.8}\text{Sr}_{0.2}\text{Cr}_{0.9}\text{Ni}_{0.1}\text{O}_3$ samples were investigated particle size of gold and chemical composition by TEM in Fig. 4. It indicates that the nanocrystallines of Au are agglomerated. The average diameter of gold particles of Au/LSCN-air and Au/LSCN-H₂ are 15.01 and 14.65 nm, respectively. Nevertheless, the gold nanoparticles are not well dispersed on the surface of perovskite.

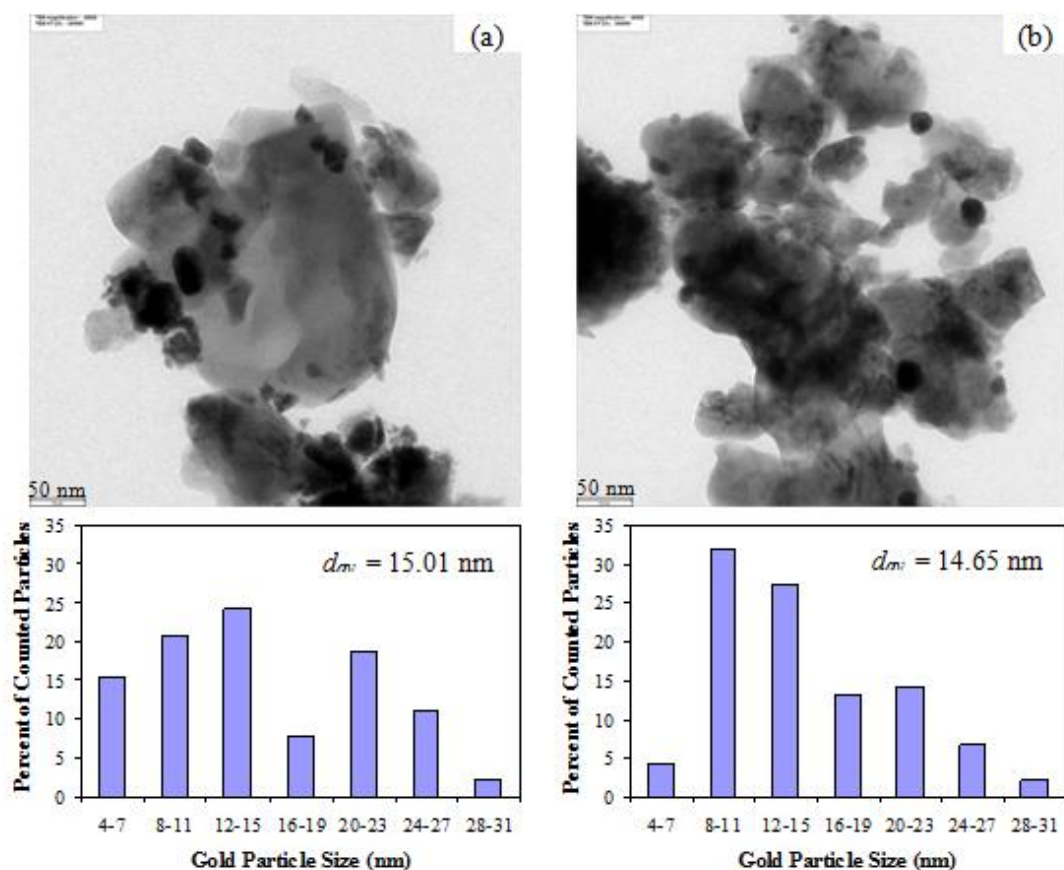


Fig. 4. TEM micrographs and gold nanoparticle size distribution of (a) Au/LSCN-air and (b) Au/LSCN-H₂.

3.2. OCM Reaction testing of LSCN and Au/LSCN

Prior the catalyst activity testing, the preliminary experiments were carried out to find optimal conditions, in which internal and external mass transfer effects are not predominant. Considering the effect of external mass transfer, the total gas flow rate was varied under a constant residence time of $5 \times 10^{-4} \text{ g} \cdot \text{min} \cdot \text{cm}^{-3}$. The reaction rate was found to be independent of the gas velocity when the gas flow rate was higher than $60 \text{ cm}^3 \cdot \text{min}^{-1}$, indicating the absence of external mass transfer effects at this high velocity. The reactions on different average sizes of catalysts were carried out in order to confirm that the experiments were performed within the region of intrinsic kinetics. It was observed that the catalysts with a particle size less than $200 \mu\text{m}$ showed no intraparticle diffusion limitation in the range of conditions studied. Therefore, in the following studies, the total flow rate was kept constant at $100 \text{ cm}^3 \cdot \text{min}^{-1}$, whereas the catalyst diameters were kept within the above-mentioned range in all experiments.

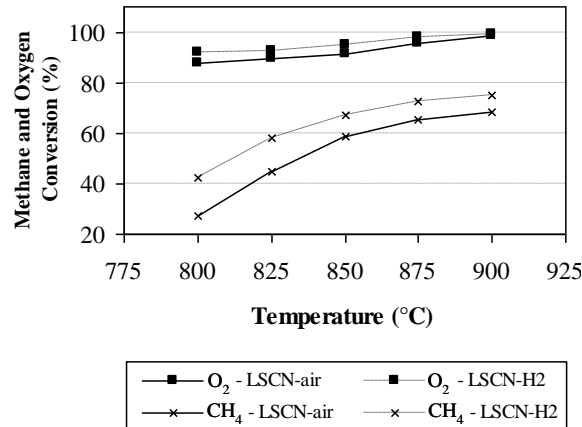


Fig. 5(a). Conversions of CH₄ and O₂ from the reactions that were catalyzed by LSCN-air and LSCN-H₂.

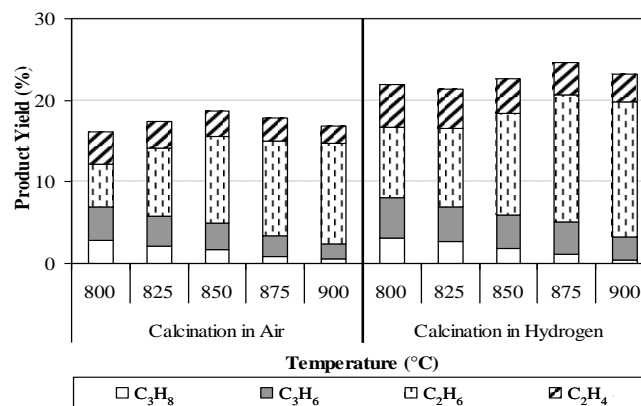


Fig. 5(b). Product yields from the reactions that were catalyzed by LSCN-air and LSCN-H₂.

LSCN-air and LSCN-H₂ were firstly studied for OCM reaction at 800, 825, 850, 875, and 900°C with a CH₄:O₂ molar ratio of 4:1. As shown in Fig. 5(a), the conversion of reactants that were catalyzed by LSCN-H₂ was higher than LSCN-air. Moreover, it was found that the conversion of reactants increased with increasing temperature. Regarding the products from the reaction, four light hydrocarbons (i.e., C₂H₄, C₂H₆, C₃H₆, and C₃H₈) and by-products were observed. The yield of light hydrocarbon production is shown in Fig. 5(b). It was found that the obtained products from OCM reaction that were catalyzed by LSCN-H₂ were higher than LSCN-air at all ranges of operating temperature studied. Furthermore, LSCN-H₂ provided C₂ hydrocarbon products more than the other one. These results corresponded to the properties of LSCN-H₂ that had higher surface area, higher porosity, and smaller particle size. In other words, the properties as mentioned before are related to the activity of OCM. Then, the amount of carbon formation on both of catalyst surfaces is determined by the Temperature Programmed Oxidation (TPO) using the mass spectrometer. The results indicate that LSCN-H₂ composed slightly higher amount of carbon (3.82 mmol/g compared to 3.48 mmol/g).

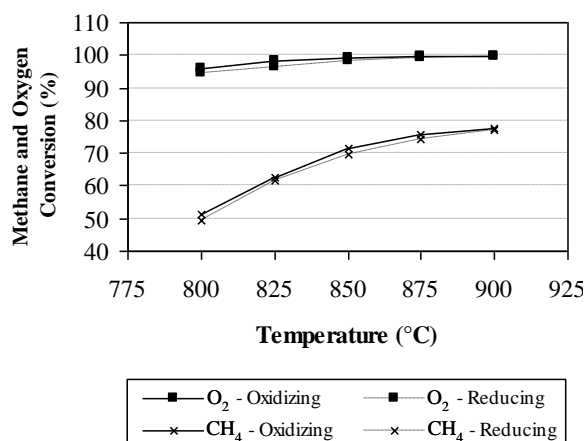


Fig. 6(a). Conversion of reactants from the reactions that were catalyzed by Au/LSCN-H2 and carried out under oxidizing and reducing conditions.

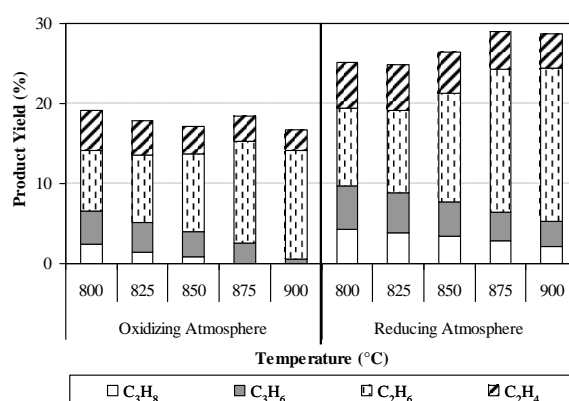
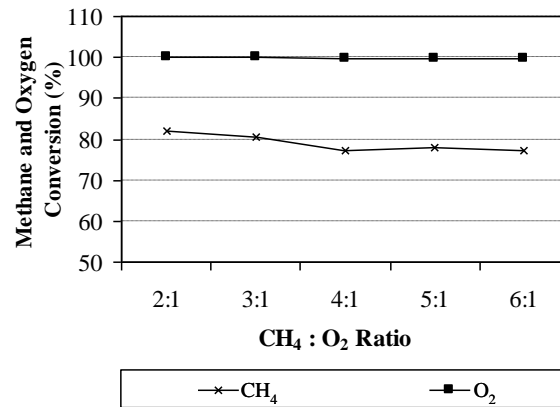
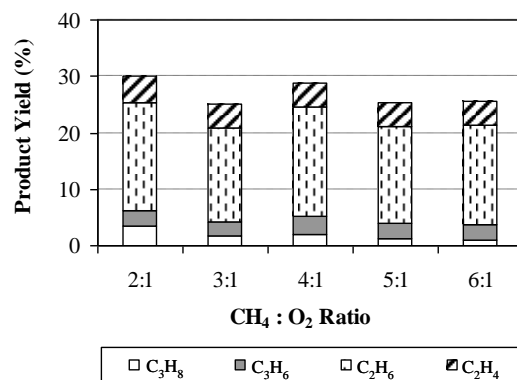


Fig. 6(b). Product yields from the reactions that were catalyzed by LSCN-H2 and Au/LSCN-H2.

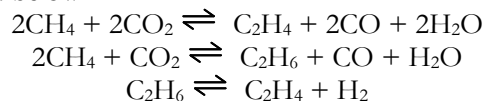
The next step, the OCM activity of LSCN-H₂ was compared to Au/LSCN-H₂ (treated under oxidizing and reducing atmospheres). The results of percent conversion of the reactants are presented in Fig. 6(a). From this figure, it was found that the percent conversion of reactants that were catalyzed by Au/LSCN (treated under oxidizing and reducing atmospheres) was relatively higher than LSCN. The product yield from Au/LSCN treated under oxidizing atmosphere was slightly lower than LSCN, whereas that from Au/LSCN treated under reducing atmosphere was higher (Fig. 6(b)). In addition, it was observed that Au/LSCN (treated under both oxidizing and reducing atmospheres) obviously reduces the carbon formation from OCM reaction. The amount of carbon species was found to decrease from 3.82 mmol/g (detected from the reaction over LSCN) to 1.95-2.03 mmol/g.

3.3. Effect of operating conditions on OCM performance of Au/LSCN-H₂

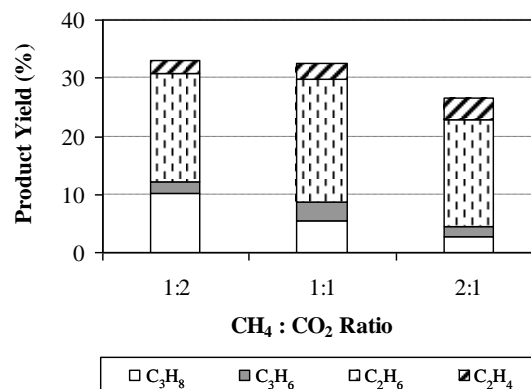
Based on all studies, Au/LSCN-H₂ was selected for the further study. Firstly, the effect of CH₄:O₂ molar ratio on the conversion and product yields was studied by varying the inlet CH₄:O₂ molar ratio from 2:1 to 3:1, 4:1, 5:1 and 6:1. As seen in Fig. 7, the conversion and the yields of light hydrocarbons production slightly decreased with increasing CH₄:O₂ ratio, which occurred from methane cracking to carbon species at too high CH₄:O₂ ratio.

Fig. 7(a). Conversion of reactants from the reactions at various CH₄:O₂ ratio.Fig. 7(b). Product yields from the reactions at various CH₄:O₂ ratio.

Then, the effect of CO₂ addition along with CH₄ (with and without the presence of O₂) was performed since Istadi and Saidina Amin (2005) has previously reported the OCM reaction between CO₂ and CH₄ to form C₂H₄ and C₂H₆ as presented below.



The evaluated CH₄:CO₂ ratios were 1:2, 1:1, and 2:1. It was found that light hydrocarbons can be generated from the reaction of CH₄ and CO₂, particularly at the CH₄:CO₂ ratio of 1:2 (Fig. 8(a)). At the CH₄:CO₂ ratio of 2:1, low light hydrocarbons were formed due to the occurring of side reaction (i.e. water gas shift reaction) to form hydrogen (Fig. 8(b)). It should be noted that, compared to the reaction of CH₄ and O₂, higher amount of C₃H₈ was produced from this reaction.

Fig. 8(a). Product yields from the reactions at different CH₄:CO₂ ratio.

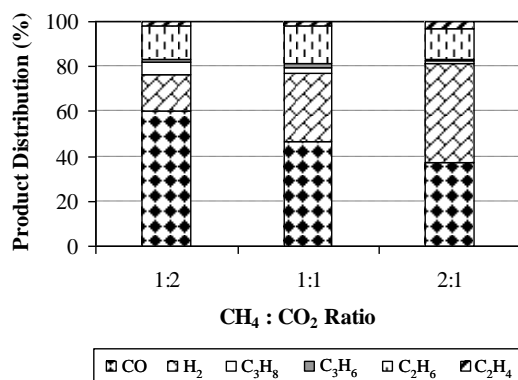


Fig. 8(b). Product distribution from the reactions at different CH₄:CO₂ ratio.

As the next step, the effect of CO₂ adding along with CH₄ and O₂ was carried out at the CH₄:O₂:CO₂ ratios of 2:1:4, 2:1:2, and 2:1:1. Similar trends as the reaction between CO₂ and CH₄ was observed as shown in Fig. 9, from which relatively high C₃H₈ was generated. Based on all studies, it can be revealed that the suitable CH₄:O₂ ratio appeared to be 2:1, from which 5.8%, 29.9%, 8.1%, and 5.8% of C₂H₄, C₂H₆, C₃H₆, and C₃H₈ can be produced respectively. Nevertheless, the content of O₂ (per inlet CH₄) showed only slight impact on the light hydrocarbons production. On the other hand, the additional of CO₂ can significantly promote the yield of C₃H₈ produced, from which the suitable CH₄:CO₂ ratio was observed to be 1:2 (with or without O₂ presenting).

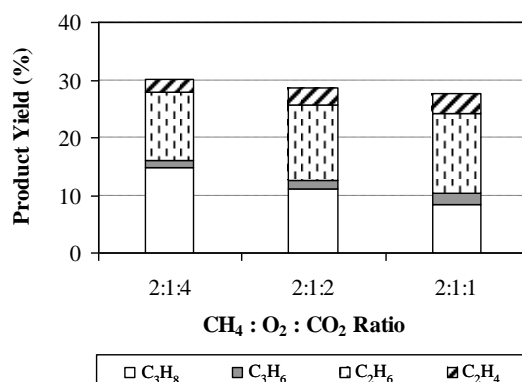


Fig. 9. Product yields from the reactions at different CH₄:O₂:CO₂ ratio.

4. Conclusion

Au supported over La_{0.8}Sr_{0.2}Cr_{0.9}Ni_{0.1}O₃ and calcined in hydrogen atmosphere was found to be the good catalyst for OCM reaction, from which C₂H₄, C₂H₆, C₃H₆, and C₃H₈ can be efficiently generated with low amount of carbon formation. According to the reaction condition, the suitable CH₄:O₂ ratio was appeared to be 2:1, from which 5.8%, 29.9%, 8.1%, and 5.8% of C₂H₄, C₂H₆, C₃H₆, and C₃H₈ can be produced. Furthermore, with or without O₂ presenting, the addition of CO₂ can significantly promote the yield of C₃H₈ produced, from which the suitable CH₄:CO₂ ratio was observed to be 1:2. Thus the above results exhibited that simultaneous generation of electrical energy and C₂ and C₃ hydrocarbon over Au/La_{0.8}Sr_{0.2}Cr_{0.9}Ni_{0.1}O₃ is possible to operate in SOFC reactor as anode catalyst for OCM reaction.

Acknowledgements

The financial support by the Joint Graduate School of Energy and Environment (JGSEE) and Thailand Research Fund (TRF) are gratefully acknowledged.

References

- [1] F. Alcaide, P. L. Cabot, and E. Brillas, "Fuel cells for chemicals and energy cogeneration," *J. Power Sources*, vol. 153, no. 1, pp. 47–60, 2006.
- [2] N. Laosiripojana, W. Wiyaratn, W. Kiatkittipong, A. Arpornwichanop, A. Soottitantawat, and S. Assabumrungrat, "Reviews on solid oxide fuel cell technology," *Engineering Journal*, vol. 13, no. 1, pp. 65–84, 2009.
- [3] W. Wiyaratn, W. Appamana, S. Charojrochkul, S. Kaewkuekool, and S. Assabumrungrat, "Au/La_{1-x}Sr_xMnO₃ nanocomposite for chemical-energy cogeneration in solid oxide fuel cell reactor," *J. Ind. Eng. Chem.*, vol. 18, no. 5, pp. 1819–1823, 2012.
- [4] W. Wiyaratn, W. Appamana, and S. Assabumrungrat, "Development of Au/La_{1-x}Sr_xMnO₃ nanocomposites for further application in a solid oxide fuel cell type reactor," *J. Ind. Eng. Chem.*, vol. 17, no. 3, pp. 474–478, 2011.
- [5] I. Istadi, S. Amin, and N. Aishah, "Co-generation of C₂ hydrocarbons and synthesis gases from methane and carbon dioxide: A thermodynamic analysis," *J. Nat. Gas Chem.*, vol. 14, pp. 140–150, 2005.
- [6] W. Kiatkittipong, T. G. Tagawa, S. Assabumrungrat, K. Silpasup, and P. Prasertthadam, "Comparative study of oxidative coupling of methane modeling in various types of reactor," *Chem. Eng. J.*, vol. 115, no. 1, pp. 63–71, 2005.
- [7] T. Tagawa, K. K. Moe, M. Ito, and S. Goto, "Fuel cell type reactor for chemicals-energy cogeneration," *Chem. Eng. Sci.*, vol. 54, no. 10, pp. 1553–1557, 1999.
- [8] S. Barison, M. Battagliarin, S. Daolio, M. Fabrizio, E. Miorin, P. L. Antonucci, S. Candamano, V. Modafferi, E. M. Bauer, C. Bellitto, and G. Righini, "Novel Au/La_{1-x}Sr_xMnO₃ and Au/La_{1-x}Sr_xCrO₃ composites: Catalytic activity for propane partial oxidation and reforming," *Solid State Ionics*, vol. 177, no. 39–40, pp. 3473–3484, 2007.
- [9] J. E. Ten Elshof, H. J. M. Bouwmeester, and H. Verweij, "Oxidative coupling of methane in a mixed-conducting perovskite membrane reactor," *Appl. Catal. B: Gen.*, vol. 130, no. 2, pp. 195–212, 1995.
- [10] Z. Fakhroueian, F. Farzaneh, and N. Afrookhteh, "Oxidative coupling of methane catalyzed by Li, Na and Mg doped BaSrTiO₃," *Fuel*, vol. 87, no. 12, pp. 2512–2516, 2008.
- [11] N. A. S. A. Istadi and S. Amin, "Synergistic effect of catalyst basicity and reducibility on performance of ternary CeO₂-based catalyst for CO₂ OCM to C₂ hydrocarbons," *J. Mol. Catal. A: Chem.*, vol. 259, no. 1–2, pp. 61–66, 2006.
- [12] E.V. Kondratenko and M. Baerns, "Oxidative coupling of methane," in *Handbook of Heterogeneous Catalysis*, G. Ertl, H. Knözinger, F. Schüth, and J. Weitkamp, Eds. Weinheim: Wiley-VCH, 2008.
- [13] G. A. Martin and C. Mirodatos, "Surface chemistry in the oxidative coupling of methane," *Fuel Process. Technol.*, vol. 42, no. 2, pp. 179–215, 1995.
- [14] J. Sfeir, P. A. Buffat, P. Möckli, N. Xanthopoulos, R. Vasquez, H. J. Mathieu, and K. Ravindranathan Thampi, "Lanthanum chromite based catalysts for oxidation of methane directly on SOFC anodes," *J. Catal.*, vol. 202, no. 2, pp. 229–244, 2001.
- [15] S. M. K. Shahri and A. N. Pour, "Ce-promoted Mn/Na₂WO₄/SiO₂ catalyst for oxidative coupling of methane at atmospheric pressure," *J. Nat. Gas Chem.*, vol. 19, no. 1, pp. 47–53, 2010.
- [16] R. Spinicci, P. Marini, S. De Rossi, M. Faticanti, and P. Porta, "Oxidative coupling of methane on LaAlO₃ perovskites partially substituted with alkali or alkali-earth ions," *J. Mol. Catal. A: Chem.*, vol. 176, no. 1, pp. 253–265, 2001.
- [17] C. Y. Yu, W. Z. Li, G. A. Martin, and C. Mirodatos, "Studies of CaTiO₃ based catalysts for the oxidative coupling of methane," *Appl. Catal. A: Gen.*, vol. 158, no. 1–2, pp. 201, 1997.
- [18] U. Berndt, D. Maier, and C. Keller, "New A^{III}B^{III}O₃ interlanthanide perovskite compounds," *J. Solid State Chem.*, vol. 13, no. 1–2, pp. 131–135, 1975.
- [19] A. Civera, M. Pavese, G. Saracco, and V. Specchia, "Combustion synthesis of perovskite-type catalysts for natural gas combustion," *Catal. Today*, vol. 83, no. 1, pp. 199–211, 2003.
- [20] C. L. Kuo, C. L. Wang, T. Y. Chen, G. J. Chen, I. M. Hung, C. J. Shih, and K. Z. Fung, "Low temperature synthesis of nanocrystalline lanthanum monoaluminate powders by chemical coprecipitation," *Journal of Alloys and Compound*, vol. 440, no. 1, pp. 367–374, 2007.
- [21] M. Lok, "Coprecipitation," in *Synthesis of Solid Catalysts*, K. P. de Jong, Ed. Weinheim: Wiley-VCH, 2009.

- [22] C. Louis, "Gold Catalysts," in *Synthesis of Solid Catalysts*. K. P. de Jong, Ed. Weinheim: Wiley-VCH, 2009.
- [23] G. Pang, X. Xu, V. Markovich, S. Avivi, O. Palchik, Y. Kolytyn, G. Gorodetsky, Y. Yeshurun, H. P. Buchkremer, and A. Gedanken, "Preparation of $\text{La}_{1-x}\text{Sr}_x\text{MnO}_3$ nanoparticles by sonication assisted coprecipitation," *Mater. Res. Bull.*, vol. 38, no. 1, pp. 11–16, 2003.
- [24] M. A. Peña and J. L. G. Fierro, "Chemical structures and performance of perovskite oxides," *Chem. Rev.*, vol. 101, no. 7, pp. 1981–2018, 2001.
- [25] A. Ruangvittayanon and S. Kuharuangrong, "Effects of Sr and Ni-dopants on the structure and conductivity of lanthanum chromite," *Advanced Materials Research*, vol. 93, pp. 558–561, 2010.
- [26] Y. L. Liu, S. Primdahl, and M. Mogensen, "Effects of impurities on microstructure in Ni/YSZ–YSZ half-cells for SOFC," *Solid State Ionics*, vol. 167, no. 1, pp. 1–10, 2004.
- [27] C. Singh and M. Rakesh, "Preparation and characterization of nickel doped, A and B site LaCoO_3 perovskites," *Indian J. Eng. Mater. Sci.*, vol. 16, no. 4, pp. 288, 2009.